Declining old pole physiology gradually enhances gene expression asymmetry in bacteria

A. M. Proenca*, M. Tuğrul, U. K. Steiner*

Evolutionary Demography Group, Institute of Biology, Freie Universität Berlin; Berlin, 14195, Germany
* correspondence: aproenca@zedat.fu-berlin.de, usteiner@zedat.fu-berlin.de

Abstract

Gene expression is a heterogeneous process at the single-cell level. This heterogeneity is often coupled to individual growth rates, which are also highly stochastic, leading to the emergence of multiple physiological states within bacterial populations. Although recent advances have shown that cellular aging acts as a deterministic driver of growth heterogeneity, the relationship between aging and the maintenance of gene expression heterogeneity is often overlooked. Here, we show that the maturation and subsequent decrease in physiological activity at the old cell poles enhances cell-to-cell phenotypic heterogeneity in *Escherichia coli*. We use single-cell microscopy and microfluidics to quantify the expression of RpoS, a transcription factor that inhibits growth while activating stress responses, throughout the aging process. By tracking mother and daughter cells over generations, we show that the maternal old poles progressively decline in their contribution towards the cellular physiology, creating a source of intracellular variance that leads to phenotypic asymmetry among mother and daughter cells. Thus, we demonstrate that gene expression, similarly to growth, is a function of the age of cell poles inherited by each cell. Our results show that the mother-daughter asymmetry is built into the declining physiology of the mother cell across generations, illustrating the deterministic nature of aging in bacterial systems. These findings provide further evidence for cellular aging as a mechanism to enhance phenotypic heterogeneity in bacterial populations, with possible consequences for stress response and survival.

Significance

Growth and gene expression are highly stochastic aspects of bacterial physiology. This heterogeneity can be advantageous for stress survival, as it creates distinct physiological states within a population. Nonetheless, the variance in growth can be partly explained by cellular aging processes, which lead to a progressive physiological decline in maternal cell lineages. Here, we show that aging also contributes to gene expression heterogeneity. As the mother cell ages, the contribution of its old poles to the production of RpoS (a growth-modulating transcription factor) declines, creating an intracellular gradient in gene expression. This gradient persists across generations, creating a physiological asymmetry between mother and daughter cells. Therefore, our findings show that the mother-daughter asymmetry that produces aging and rejuvenation patterns in a bacterial population is built into the intracellular asymmetry of mother cells. These findings offer insights on the maintenance of phenotypic heterogeneity in bacterial populations, which has implications for stress survival.

Introduction

Within isogenic populations, individual cells exhibit heterogeneity in gene expression and growth rates. This physiological variability often results from the propagation of stochastic fluctuations across regulatory networks (1, 2), leading to the coexistence of distinct physiological states within populations (3, 4). In bacterial populations, for example, such gene expression fluctuations can lead some individuals to reproduce more quickly while others enter a slow-growing or dormant state (5). Rather than being detrimental for the population, this physiological heterogeneity is closely tied to survival in stressful conditions or changing environments (6–8). Nonetheless, recent studies have demonstrated that deterministic factors, such as cellular aging, also contribute towards the phenotypic heterogeneity previously attributed to stochasticity alone (9, 10).

Aging, a physiological decline over time (11, 12), propagates along bacterial lineages across generations. According to classic theories, aging requires a clear separation between the soma and germline (13), or at least some degree of asymmetry among them (14). The fact that bacteria usually divide with morphological symmetry has, consequently, led to the assumption that these organisms should flee aging (13, 15, 16). However, the notion of symmetric fission in unicellular organisms has been overhauled in the last decades (17–20). In rod-shaped bacteria, despite their apparent morphological symmetry, aging is determined by the asymmetric inheritance of cell poles. Bacteria must synthesize a new pole at the central plane after each fission. In the following division, one cell inherits this newly formed pole, while the other receives an old pole that can be inherited over many generations (Figure 1A). The deterministic inheritance of old poles correlates with reduced growth, lower division rates, and increased mortality, whereas the inheritance of new poles leads to higher fitness (17, 18, 21, 22). The resulting physiological heterogeneity likely drives the variation in demographic fates among cells of identical genetic background in the same environment (Jouvet et al., 2018). In fact, when populations experience extrinsic stress, the inheritance of old poles leads to a higher probability of death, while new-pole cells continue to proliferate (23). It is therefore reasonable to assume that cells receiving the old pole progressively accumulate an "aging factor", which is asymmetrically partitioned upon division (24). This process may be described as a mother cell that ages while producing a new daughter cell at each fission event. Here we will adhere to this perspective, as it refers back to the concept of separation between soma and germline (25) and simplifies the definition of aging at the single-cell level.

A possible mechanism of this physiological heterogeneity is the asymmetric partitioning of intracellular damage (21, 26, 27). Misfolded proteins, for instance, tend to accumulate in the form of aggregates that eventually become too large to diffuse across the nucleoid, thus becoming trapped at the cell poles (28–30). The inheritance of protein aggregates has been shown to negatively correlate with growth rates (28, 31), but more recent studies suggest that other factors must be involved in bacterial aging. Large protein aggregates are generally absent in unstressed populations (32), and yet the physiological distinction between mothers and daughters is observed in healthy cells (10, 33). In addition, for cells under heat stress, the rejuvenation of the daughter depends on the chronological age of the mother (22), indicating that daughters can inherit intracellular damage not associated with

old poles. These results suggest that, besides damage partitioning, other intracellular mechanisms also contribute to the physiological asymmetry between mother and daughter cells.

Sources of physiological heterogeneity that are considered purely stochastic can provide hints of mechanisms that influence bacterial aging (34). Gene expression, for example, is regarded as highly stochastic at the single-cell level (2, 8, 35), but recent evidence suggests that newly synthesized gene products are partitioned with deterministic asymmetry towards daughter cells (36). It remains unclear how this pattern behaves over time, and whether it can be extended to the expression of growth-modulating transcription factors. For instance, RpoS, a sigma factor that coordinates the general stress response and stationary phase transitioning in *Escherichia coli* (37, 38), is expressed with large stochasticity during exponential growth (4, 8). This transcription factor regulates about 10% of *E. coli* genes (39), inhibiting cellular growth and increasing the variability in physiological states within the population (4). If growth-modulating factors also correlate with the inheritance of old poles and asymmetric growth physiology, it could reveal another mechanism of cellular aging.

Here we address these issues by exploring the dynamics of RpoS expression associated with bacterial aging. Since it inhibits growth, a straightforward hypothesis would be that mother cells have higher RpoS expression than their daughters, and that RpoS levels would increase as the mother ages as a response to intracellular stress. We demonstrate that, unexpectedly, daughter cells have RpoS higher expression despite also growing faster than mother cells. This asymmetry increases the gene expression heterogeneity of the population, indicating that both deterministic and stochastic factors contribute towards the total variability. Moreover, we show that gene expression asymmetry is built into the intracellular environment of the mother cell. As the cell ages, the contribution of its old pole towards the overall physiology of the cell decreases, creating intracellular asymmetry in RpoS expression. Thus, cellular aging produces patterns of gene expression asymmetry that enhance the phenotypic heterogeneity found within bacterial populations.

Results

Mother and daughter cells have asymmetric RpoS expression

To investigate the effects of divisional asymmetry on gene expression and growth heterogeneity, we imaged single *E. coli* cells encoding a fluorescent transcriptional reporter of the RpoS promoter activity (P_{rpoS}-*GFP*). Cell populations were grown in constant exponential phase in the mother machine microfluidic device (40). These devices contain thousands of narrow growth wells connected in one end by flow channels, which supply fresh nutrients to trapped cells (Figure 1A). Throughout the experiments, the mother cell remains lodged at the closed end of the growth well, while continuously producing daughter cells. We tracked mother cells for one hundred generations and each daughter from birth to its first division, quantifying aspects of their growth physiology (length, division intervals, elongation rates) and RpoS expression (mean fluorescence intensity) while growing in the absence of extrinsic stress.

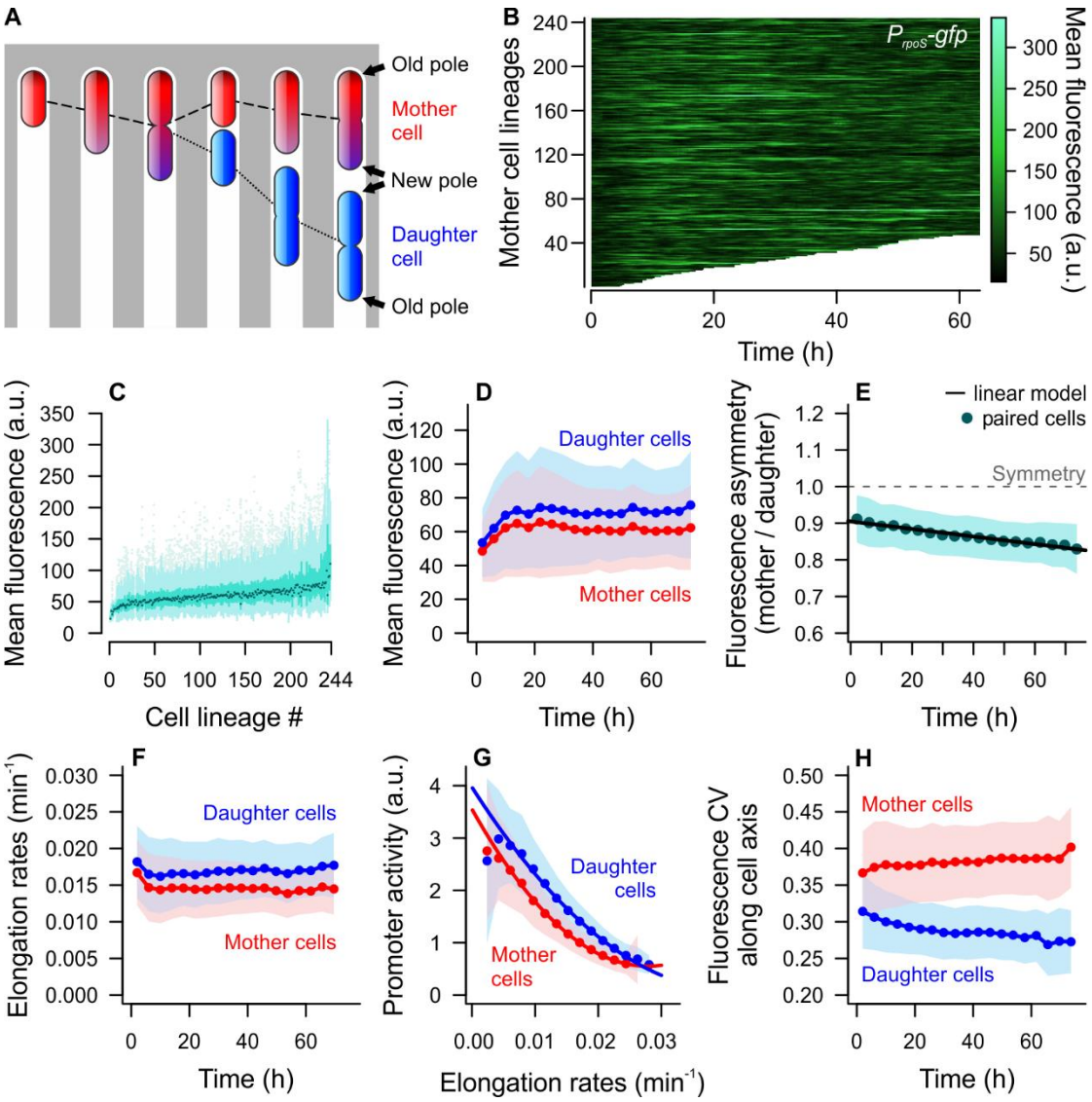

Figure 1. RpoS expression reveals both stochastic and deterministic variance. (A) Graphical representation of bacterial cells growing the mother machine device. Old cell poles, inherited by mother cells with each division, remain trapped at the closed end of growth wells. When the mother divides, it produces a daughter cell that inherits its new pole. (B) RpoS expression heatmap of 244 mother cell lineages, showing stochastic fluorescence pulses over time. Mother cells were sorted by longevity, with interrupted lines representing cells that died or were washed away. (C) Boxplots of cells observed within each growth well, pooling mothers and daughters, indicate large among-lineage heterogeneity. (D) Besides the stochastic variance contributing for differences among mother cells and gene expression fluctuations, the asymmetry between mothers and daughters contributes to the total variance of RpoS expression. (E) Asymmetry increases over time, when considering mother-daughter pairs observed shortly after division. (F) This physiological difference is also present for elongation rates, with daughters displaying faster growth. (G) RpoS promoter activity and growth showed a negative correlation, but daughters displayed both faster growth and higher promoter activity. (H) Mothers and daughters also differed in the intracellular variance of RpoS signal. (D to H) Bins represent mean ± SD.

Across mother cell lineages, we observed highly stochastic RpoS expression (Figure 1B). Random peaks of promoter activity over time — transcriptional bursting — corresponded to periods of slow growth and shorter cell lengths (Figure S1), confirming that bursts of RpoS activity can lead to transient growth inhibition during exponential phase (4). The heterogeneity of RpoS expression was further demonstrated by the long tail of mean fluorescence and promoter activity distributions (Figure

S1B and S1D). The distributions themselves differed among the observed lineages (Figure 1C), with mean fluorescence values ranging from 24.65 ± 5.04 to 112.70 ± 37.98 a.u. (mean ± SD). A simple sum of squares partitioning attributed 16.9% [CI: 16.7-18.1%] of the total variance to this among-lineage heterogeneity, which might be explained by the initial state of each mother cell (*e.g.,* intracellular damage, age, etc.) and stochastic differences among lineages. Although the starting population in the mother machine is predominantly young, since all cells were loaded from exponential cultures (22), this among-lineage variance partly derives from some mother cells exhibiting longer RpoS transcriptional bursts, as we can see in Figure 1B. Most of the remaining variance was entirely stochastic (56.4% [CI: 55.4-56.9%]), and the factors comprising the other 26.7% (*e.g.*, growth and asymmetry) will be addressed in detail below. These random bursts of transcriptional activity and among-lineage heterogeneity confirm previous findings on the stochasticity of RpoS expression at the single-cell level (4).

Beyond this large stochastic variance, we observed that the phenotypic heterogeneity within populations was magnified by the physiological asymmetry between mother and daughter cells (Figure 1D). Daughter cells consistently displayed higher mean fluorescence (69.9 ± 30.0 a.u.) than their mothers (60.7 ± 26.5 a.u.; Wilcoxon signed-rank test, V = 812,808, $p < 0.001$). To be certain that this pattern was due to aging and not an artifact of the positioning of cells in the growth wells, we measured the asymmetry after the first cell division recorded within the device (Figure S2). At this early point, it is not yet possible to know which cell inherits an old or new pole after division. As expected, asymmetry was absent on the first division and gradually appeared on the subsequent generations, indicating that this pattern has a physiological source. This hypothesis was supported by the fact that asymmetry increased over time (Figure 1E; n = 18,970 mother-daughter pairs, t = -49.52. $p < 0.001$, $R^2 = 0.12$), suggesting an aging effect on RpoS activity. In fact, by proceeding with the partitioning of the RpoS expression variance, we observed that 9.0% [CI: 8.4-9.3%] was due to the mother-daughter asymmetry.

Interactions between RpoS expression and growth, as reported for mother cells in Figure S1, were also present when comparing mothers and daughters. At the population level there was a negative correlation between growth and RpoS activity (Figure 1G), which accounted for 17.7% [CI: 16.9-18.2%] of the variance in gene expression. When considering mothers and daughters separately, however, daughter cells showed faster elongation rates despite also exhibiting higher RpoS signal (Figure 1F; paired t test, t = 122.98, $p < 0.001$). Even when displaying similar elongation rates to mother cells, daughter cells exhibited higher promoter activity (Figure 1G), which suggests that the difference in overall metabolic rates cannot explain the observed asymmetry. Since growth and RpoS are mutually inhibitory (4), it is possible that daughter cells dilute the RpoS signal through faster elongation, whereas mother cells are more sensitive to this inhibitory signal.

More importantly, our results suggested a core distinction between mother and daughter cells that cannot be captured by the quantification of mean physiological attributes. By measuring the variation in fluorescence levels across the cell length (*i.e.*, from old to new pole), we observed that mothers harbored much larger intracellular variation (Figure 1H; paired t-test, t = 259.47, $p < 0.001$),

and this distinction increased over time. This difference in intracellular variance might help elucidate the source of asymmetry in RpoS expression and will be further explored in the following section.

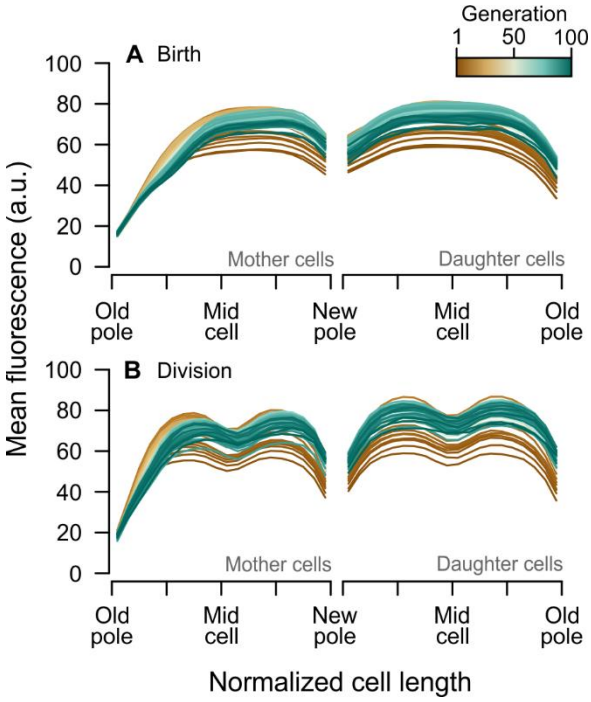

Figure 2. Asymmetric RpoS expression across the cell length. Each line represents a series of fluorescence measurements from pole to pole, averaged for all cells of a given generation. Mother cells (left) had darker areas around the old poles from birth (A) to division (B), indicating a gradient in RpoS expression along the cell length. Daughter cells, on the other hand, showed higher intracellular homogeneity in gene expression. The fission site was visible in the transects measured before division. See also Figure S3.

Mother-daughter asymmetry is built within the mother cell

To investigate the intracellular distribution of RpoS, we quantified the mean fluorescence signal along the cell axis of each individual. Cells were normalized by length to allow for the comparison of these distributions, and average fluorescence transects were calculated for each generation (Figure 2). The resulting transects indicated that the RpoS heterogeneity observed across mother cells derives from a gradient in gene expression between new and old poles. We evaluated these gradients through generalized additive models, considering the distance from each pole towards the center and the time of each measurement (in generations) as smooth terms (see Figure S3, Table S1 and S2). Our analysis indicated that the effect of distance from the pole varied smoothly with time ($p < 0.001$). Additionally, RpoS levels in each half of the mother cell varied differently over time ($p < 0.001$) and across the cell length ($p < 0.001$). Together, these factors explained 51.3% of the deviance in RpoS expression. Daughter cells exhibited a more homogeneous distribution of intracellular fluorescence, with old poles showing slightly lower fluorescence levels (Figure S3 and Table S2). Although our statistical models indicated a significant difference between new and old areas of the cell ($p < 0.001$), each varying smoothly across length ($p < 0.001$) and over time ($p < 0.001$), these factors could only explain 11.7% of the deviance in daughter cell RpoS expression. This intracellular asymmetry persisted throughout each cell cycle, as shown in Figure 2B. The fission plane

becomes visible halfway through the generation as a dip in RpoS signal, confirming that these measurements reflect the level of intracellular physiological activity. The intracellular asymmetry that an individual exhibited prior to division was correlated with the asymmetry among its offspring (Figure S3), indicating that this pattern propagates across generations.

Pole age determines intracellular gene expression asymmetry

Since mother cells exhibit a gene expression gradient, and the RpoS asymmetry between mothers and daughters increases over time (Figure 1E), we can hypothesize that the intracellular heterogeneity of mother cells is age dependent. In bacteria, this age is a function of how many times a cell pole was consecutively inherited (Figure 3A). While maternal old poles exist for up to 100 generations in our experiments ($0 < \text{age} < 100$), their new poles are always synthesized at the last fission event (age = 0). The new pole of the daughter cell, consequently, also has age = 0, while its old pole has age = 1. As such, we expect old poles of mother cells to be physiologically older, but new poles of mothers and daughters should be equivalent. This is demonstrated through fluorescence measurements in Figure 3. Maternal old poles exhibited lower RpoS expression, with mean fluorescence 18.9 ± 11.9 a.u. lower than old poles of daughter cells (Figure 3B; $t = 85.387$, $p < 0.001$). RpoS levels in new poles, on the other hand, differed only by 1.1 ± 4.7 a.u. (Figure 3C; $t = 5.925$, $p < 0.001$). The greater homogeneity of daughter cells can also be visualized through the ratios between new and old poles (Figure 3D), which approach 1 over time. These ratios varied smoothly over time for both mothers ($F = 540.48$, $p < 0.001$) and daughters ($F = 54.96$, $p < 0.001$), with a generalized additive model indicating that these terms account for 70.8% of the deviance in intracellular asymmetry. Mother cells exhibited increasing intracellular asymmetry with age, which coincides with the increasing age difference between its old and new poles.

The mother machine design allows us to extend this prediction for another pair of cells, represented in Figure 3A. When a daughter cell divides, its old and new poles age by one generation as they are inherited by the offspring. Daughter 2 inherits the new pole, now age = 1, while Daughter 3 receives the old pole (age = 2). It is important to look at these cells to determine how quickly intracellular asymmetry is built across generations — *i.e.*, whether the lapse of a single generation can produce physiological asymmetry between cell poles. Our results confirmed this hypothesis (Figure 3E), with Daughter 3 exhibiting lower levels of RpoS expression on its old pole (mean ratio = 92.64%; new vs old pole paired t test: $t = 132.5$, $p < 0.001$). Furthermore, since Daughter 3 is positioned closer to the opening of the growth well and surrounded by neighboring cells (Figure S4), the fact that it also displays intracellular asymmetry further demonstrates that this phenomenon has a physiological origin rather than being an imaging artifact. Taken together, these results suggest that RpoS expression gradients across each cell are correlated with the age of its cell poles, and these intracellular gradients translate into asymmetric gene expression among the offspring upon division.

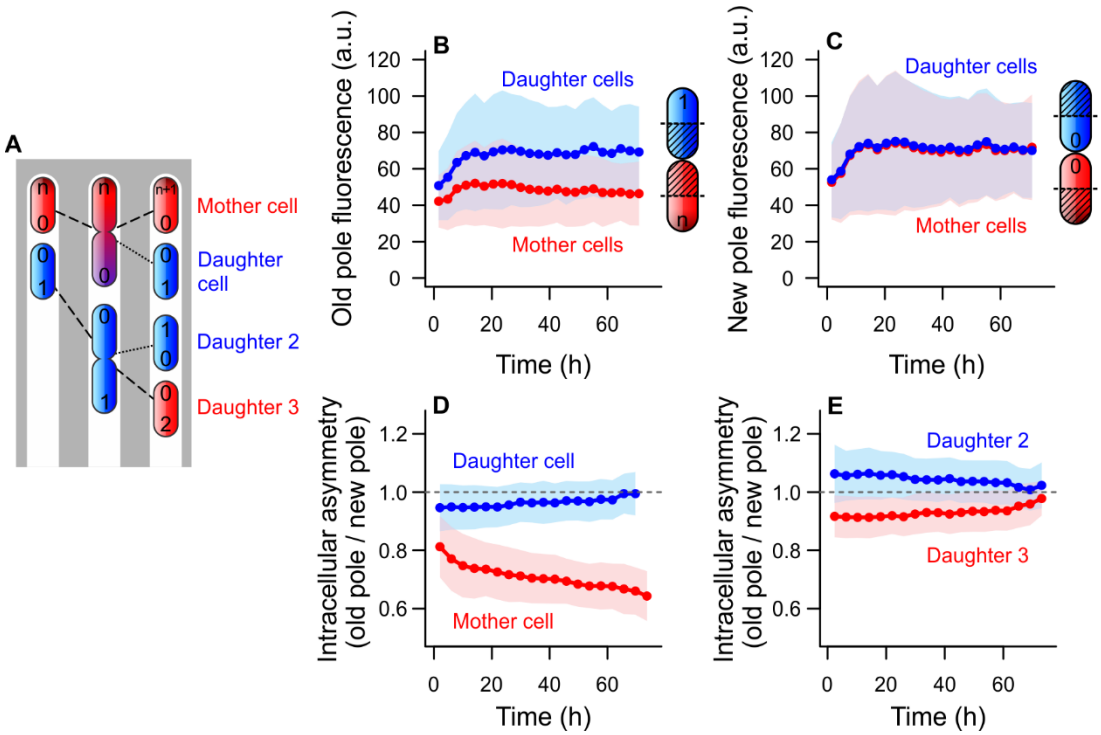

Figure 3. Intracellular asymmetry depends on the age of cell poles. (A) Graphical representation of cell polarity in the mother machine device. Maternal old poles become older with each generation, while old poles of daughter cells always have age = 1. When this daughter divides, it produces Daughter 3, inheriting the old pole, and Daughter 2, which receives the new pole. (B) This difference in pole ages predicts that most of the difference between mother and daughter cells should come from their old poles. In fact, old poles of daughter cells (n = 18,445) exhibited higher RpoS expression than maternal old poles (n = 18,979). (C) In contrast, new poles of mother and daughter cells show little difference in RpoS expression over time, since they were both synthesized at the fission site. (D) As the maternal old pole ages, the intracellular asymmetry of mother cells increases. Daughter cells remain nearly symmetric over time. (E) Some level of intracellular asymmetry is visible in Daughters 2 and 3, with Daughter 3 showing lower RpoS expression in the old pole area despite it being only two generations old. Bins represent mean ± SD.

Aging poles lead to physiological decline

To determine the effects of bearing old poles on the physiology of mother cells, we calculated the length of these poles based on RpoS expression gradients (Figure 2A). For each cell, we performed a segmented regression analysis to find the breakpoint that determined the transition from the polar gradient to the mid-cell fluorescence plateau. The distance from the cell pole to this breakpoint represents the old pole length, shown in Figure 4A. Both the old pole length ($t = 84.44$, $p < 0.001$) and the overall cell length ($t = 47.37$, $p < 0.001$) increased over time, though at distinct rates (ANCOVA interaction: $F = 87.08$, $p < 0.001$). Combining these measurements, we observed an increase in the fraction of the mother cell represented by the old pole ($m = 0.0015$, $t = 50.82$, $p < 0.001$), from 25.3% to 36.2% after 72 h (Figure 4B). To determine whether these changes could explain the mother-daughter physiological asymmetry, we recalculated the estimates of RpoS activity on mother cells while excluding the old pole area (Figure 4C and 4D). Both mean fluorescence ($t = 28.31$, $p < 0.001$) and promoter activity ($t = 10.87$, $p < 0.001$) increased, with the former approaching daughter cell levels. The fact that promoter activity remained asymmetric despite the removal of old poles indicates that other factors, such as elongation rates, remain an essential component of

bacterial asymmetry. Taken together, these results indicate that increasingly aged old poles promote the gradual physiological decline of mother cells, since these areas have lower contribution to the overall gene expression.

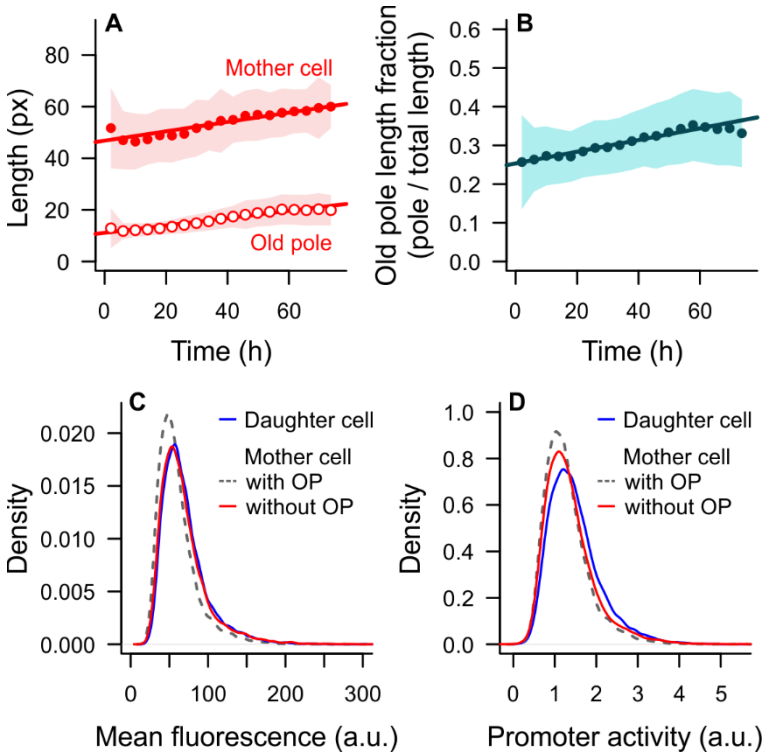

Figure 4. Old pole area contributes to physiological decline. (A) Mother cells increase in birth length over time, which is accompanied by an elongation of the old pole area of the cell. (B) With age, old poles represent an increasingly larger proportion of the mother cell. (A and B) Bins represent mean ± SD. (C and D) When old poles are removed and RpoS activity recalculated, it approaches the levels of daughter cells. This suggests that bearing old poles contributes to the lower gene expression observed in mother cells.

Discussion

Gene expression, just like growth, is highly stochastic in bacteria. Nonetheless, we demonstrated that part of the variation commonly attributed to stochastic factors is due to cellular aging. Mother cells, those inheriting old poles with every passing generation, showed lower levels of RpoS activity despite also growing more slowly than their daughters. These differences could not be explained by the higher metabolic rates of daughter cells, since asymmetry was present even when mothers and daughters elongated at similar rates, but rather by cellular aging. An asymmetry gradient within the mother cell was produced by the age difference between its new and old poles, which manifested the next generation as the asymmetry between mother and daughter. The daughter cell, which has poles of similar age, exhibited homogeneous RpoS expression. Still, because mother cells showed lower elongation rates, it is likely that these aging mothers have higher sensitivity to the growth-inhibitory activity of RpoS.

A comparable paradigm shift occurred when the influence of cellular aging over the distribution of bacterial growth states was demonstrated. Although bacteria grow at a constant rate

when maintained in stable environmental conditions (40, 41), mother and daughter cells reach distinct states of growth stability (10), building on the notion that the inheritance of old cell poles leads to lower fitness (17, 18, 28). This deterministic asymmetry can be advantageous over the purely stochastic partitioning of damaged components (9, 42). Nonetheless, stochastic components have a core relevance for bacterial physiology, dictating mortality patterns of mother and daughter cells (22), and propagating through genetic regulatory networks (1, 2). The activity of transcription factors such as RpoS is no less stochastic, with pulsating dynamics of growth inhibition that can lead to higher stress survival (4, 8, 43). By showing that mother and daughter cells have asymmetric RpoS expression, our results suggest yet another layer to the phenotypic heterogeneity modulated by this sigma factor. It remains an open question whether the higher levels of RpoS observed in daughter cells could also be involved in their higher probability of survival to oxidative stresses (23).

The evidence that asymmetry is also present at the gene expression level also invites a new mechanistic perspective on bacterial aging that links molecular to organismal processes. The aging phenotype of mother cells has been mostly attributed to the accumulation of misfolded proteins (10, 28, 30, 31). However, recent studies have suggested that the inheritance of protein aggregates does not always correlate with slower growth rates (32, 33), indicating that other factors must contribute to the phenotypic asymmetry between mother and daughter cells. For instance, Shi *et al.* have demonstrated that daughter cells receive more newly synthesized proteins upon division (36), although this study was limited to a few generations. Our results suggest that, beyond simply inheriting more new genetic products, daughter cells have higher gene expression rates. By quantifying growth and RpoS expression for 100 generations, we demonstrated that the maternal old pole shows a continuous decrease in contribution to the overall physiology of the cell, even when elongation rates did not capture such decline. These patterns might be explained by the asymmetric partitioning of ribosomes upon divisions, with daughter cells inheriting a larger fraction of maternal ribosomes (44).

We have shown that cellular aging contributes to the phenotypic heterogeneity found within bacterial populations, influencing growth and gene expression. More than producing a fixed asymmetry between mothers and daughters, the progressive aging of old poles widens the physiological heterogeneity with each division. By linking gene expression and aging dynamics, our findings provide a framework for future studies on the causal understanding of bacterial aging. Moreover, our results invite the question of which other mechanisms of metabolic regulation might be involved in the aging process. It is possible that the maturation and physiological decline of the old poles have direct consequences for bacterial growth — *e.g.*, the old area, representing a considerable fraction of the mother cell, might have a lower contribution to cell wall elongation, producing differences in elongation rates among mother and daughter cells. Taken together, our findings demonstrate that cellular aging is an essential part of non-genetic variance in bacterial populations, and future studies might elucidate its role as a driver of phenotypic heterogeneity involved with survival to oxidative stress and antibiotic treatments.

Materials and methods

Strains and growth conditions

E. coli K-12 strain MG1655 containing a plasmid-based GFP reporter of RpoS expression was obtained from the U. Alon library (45). An extensive characterization performed by Patange et al. (4) demonstrated that the RpoS activity patterns observed on a plasmidial reporter do not differ from a chromosomally integrated one, except for a lower fluorescence intensity on the latter. Since imaging strains with a chromosomal integration would require higher exposure to phototoxic stress, we used the original strain to minimize damage exposure. Liquid cultures were performed on M9 media (1xM9 salts, 2 mM $MgSO_4$, 0.1 mM $CaCl_2$) supplemented with 0.2% Casamino Acids and 0.4% glucose. For microfluidic experiments, 0.075% Tween20 (Sigma-Aldrich) and 1 µg/ml Propidium Iodide (PI) were added to the media. Tween20 prevents cell adhesion to the walls of a microfluidic device, and PI is a marker of cell lysis. All experiments were conducted at 37°C.

Microfluidic design and fabrication

The mother machine microfluidic design was used for cell capture and single-cell imaging (40). The design consisted of four parallel flow channels (1 cm x 80 µm x 10 µm), each containing 1,000 growth wells (25 x 0.8 x 1.2 µm). Each growth well contains a mother cell lineage, which receives fresh culture medium diffused from the flow channels throughout the experiment. The original mold was fabricated through laser etching, and epoxy copies were produced for constant handling. Individual devices were fabricated with Sylgard 184 polydimethylsiloxane (PDMS) (Dow Corning, USA) using epoxy copies as negative molds for PDMS casting. The cast was degassed in a vacuum chamber and hardened at 80°C for 1h, then removed from the mold and punctured with a 0.5 mm biopsy punch to create inlet and outlet ports. Each device was thoroughly washed with ethanol and water, dried, and attached to 24 x 40 mm coverslips through plasma bonding. A final curing step was performed by incubating bonded devices at 60°C overnight. Prior to use, devices were plasma-activated and treated with 20% polyethylene glycol (PEG) for 1 h.

Cell loading and device setup

Overnight bacterial cultures were diluted into 15 ml M9 media and grown to exponential phase for 2 h prior to loading (until OD_{600} = 0.4-0.6 was reached). Cultures were centrifuged at 4000 rpm for 10 min, then resuspended into 200 µl of M9+Tween20+PI. These concentrated cultures were injected into the devices through the outlet ports, and devices were centrifuged at 1500 rpm for 8 min to push bacteria into the growth wells. Once the proper loading was verified, the flow media input was connected to each device through Tygon tubing (ND 100-80, Saint-Gobain, Darwin Microfluidics). A constant flow of 200 µl/h was ensured by a peristaltic pump (Ole Dich, Denmark). In the segment of the inlet tubing that ran through the pump, Tygon tubing was replaced by flexible pumping tubing (Masterflex Tygon E-3603, VWR). Outflow tubing were connected to outlet ports, running to a waste

container. Loaded devices were placed in the microscopy incubation chamber at 37°C (Pecon TempController 2000-1).

Microscopy and image acquisition

Time-lapse imaging was performed on a Nikon Eclipse Ti2 inverted microscope equipped with a motorized stage and Perfect Focus System (PFS), using a 100x oil objective and DS-Qi2 camera. Automated image acquisition was controlled through the NIS Elements software, configured for phase contrast acquisition in 2 min intervals for 72 h. In order to decrease photooxidation effects (23), fluorescence images for GFP (200 ms exposure, 1% intensity) and RFP (300 ms, 2% intensity) quantification were obtained in 10 min intervals.

Image processing

Images were pre-processed on ImageJ for chromatic shift correction and background subtraction (rolling ball radius = 20 px, sliding paraboloid). Automated image processing was performed using the DeLTA deep learning-based software (46), for which the deep learning algorithm was further trained on diverse single-cell data from our experimental system. Segmentation was performed on phase contrast images, and measurements were obtained for cell length, area, division intervals, and mean fluorescence intensity. Fluorescence transects were obtained by extracting the mean fluorescence intensity of each pixel along the mid-cell line. Segmentation and tracking errors, though rare, were corrected with a custom program implemented in R v.4.1.2 (47). Manual corrections were performed when necessary. Each lineage was followed until the death of the mother cell, and only complete generations were considered for statistical analyses (*i.e.,* daughter cells that left the growth well before a division was observed were excluded from measurements).

Statistical analysis

Statistical analyses on the output growth and fluorescence data were performed in R v.4.1.2, considering mother cells for the entirety of the experiments and the first generation of each daughter cell. For the comparison of individuals at the same stage of the cell cycle, fluorescence measurements were taken from the first frame after division (indicated as “birth” frame on Figure 2) unless otherwise indicated. Elongation rates were calculated for each cell from an exponential fit to length measurements of each generation. As such, mean fluorescence and elongation rate estimates for mothers and daughters are paired for every division. When parametric tests on fluorescence data were necessary, the data was log-transformed. On all representations of binned data, bins represent mean ± standard deviation (SD), and bins comprising fewer than 10 measurements were excluded.

Fluorescence transects shown in Figure 2 were normalized by length for graphical representation and for analysis through generalized additive models, which were performed using R

package mgcv v.1.3-38 (48). While the transects in the main figure were averaged for each generation, individual measurements were used in the analysis. We focused on the differences between new and old cell areas for the construction of the models, as shown in Table S1. Each fluorescence transect was cut in half, thus splitting the new and old areas of each cell, and the distance from the pole towards the center was used as a smoothing term in the model (see also representation in Figure S3A and B). The model structure that provided the lowest AIC was considered optimal (Table S1) (49). On analyses quantifying differences in intracellular asymmetry, such as shown in Figure 3, raw measurements were used without the need for length normalization.

These transects were also used to obtain the proportion of the mother cell represented by the old area, shown in Figure 4. In this case, each log-transformed transect was fit with a segmented regression using R package “segmented” v.1.4-0 (50). The breakpoint along the cell length marking the transition from the gradient to the fluorescence plateau was used as the old pole length in further analyses.

Promoter activity quantification

The estimate of RpoS promoter activity was performed as previously described (4, 8). Given the mean fluorescence of a cell (M), its length (L) and a constant (p = 0.02), promoter activity (A) is defined as

$$A = M\left(\frac{1}{L}\frac{dL}{dt} + p\right) + \frac{dM}{dt}$$

The promoter activity of mother cells over time was performed for all fluorescence measurements throughout the individual’s lifespan. In this case, M was smoothed with a moving window of 5 fluorescence frames, and the resulting A was again averaged over a similar moving window for graphical representation. For the comparison of mother and daughter cells, since the latter was only followed for a generation, measurements (M and L) at the beginning and end of each generation were used to obtain A. No data smoothing was employed in this comparison.

Data availability

All data and supporting code will be available from a public repository by the time of publication. Strains can be obtained from the Uri Alon library of *E. coli* fluorescent transcriptional reporters (45) and materials will be shared upon request.

Acknowledgements

We thank the Evolutionary Demography Group members, L. Stäcker and J. Kuom for experimental support, and Dr. A. Nath for discussions and feedback. AMP was supported by a

Humboldt Research Fellowship provided by the Alexander von Humboldt Foundation and by the Rising Star Fellowship (Freie Universität Berlin). MT was funded by the German Research Foundation (DFG, 430174701) and by the European Union under the Marie Skłodowska-Curie Actions' European Postdoctoral Fellowship grant agreement (101069035). UKS was funded by the German Research Foundation (DFG, 430170797) as a Heisenberg Fellow.

References:

1. A. Urchueguía, *et al.*, Genome-wide gene expression noise in Escherichia coli is condition-dependent and determined by propagation of noise through the regulatory network. *PLoS Biol.* **19**, e3001491 (2021).

2. N. Rosenfeld, J. W. Young, U. Alon, P. S. Swain, M. B. Elowitz, Gene regulation at the single-cell level. *Science* **307**, 1962–5 (2005).

3. C. Wu, *et al.*, Cellular perception of growth rate and the mechanistic origin of bacterial growth law. *Proc. Natl. Acad. Sci. U. S. A.* **119**, 1–9 (2022).

4. O. Patange, *et al.*, Escherichia coli can survive stress by noisy growth modulation. *Nat. Commun.* **9** (2018).

5. N. Q. Balaban, J. Merrin, R. Chait, L. Kowalik, S. Leibler, Bacterial persistence as a phenotypic switch. *Science.* **305**, 1622–1625 (2004).

6. O. Gefen, N. Q. Balaban, The importance of being persistent: Heterogeneity of bacterial populations under antibiotic stress. *FEMS Microbiol. Rev.* **33**, 704–717 (2009).

7. P. B. Rainey, *et al.*, The evolutionary emergence of stochastic phenotype switching in bacteria. *Microb. Cell Fact.* **10**, S14 (2011).

8. N. M. V. Sampaio, C. M. Blassick, V. Andreani, J. B. Lugagne, M. J. Dunlop, Dynamic gene expression and growth underlie cell-to-cell heterogeneity in Escherichia coli stress response. *Proc. Natl. Acad. Sci. U. S. A.* **119**, 1–12 (2022).

9. L. Chao, C. U. Rang, A. M. Proenca, J. U. Chao, Asymmetrical Damage Partitioning in Bacteria: A Model for the Evolution of Stochasticity, Determinism, and Genetic Assimilation. *PLoS Comput. Biol.* **12**, e1004700 (2016).

10. A. M. Proenca, C. U. Rang, C. Buetz, C. Shi, L. Chao, Age structure landscapes emerge from the equilibrium between aging and rejuvenation in bacterial populations. *Nat. Commun.* **9**, 3722 (2018).

11. S. C. Stearns, The Evolution of Life History Traits: A Critique of the Theory and a Review of the Data. *Annu. Rev. Ecol. Syst.* **8**, 145–171 (1977).

12. M. R. Rose, *Evolutionary Biology of Aging* (Oxford University Press, 1991).

13. T. B. L. Kirkwood, Evolution of ageing. **270**, 301–304 (1977).

14. L. Partridge, N. H. Barton, Optimally, mutation and the evolution of ageing. *Nature* **362**, 305–311 (1993).

15. G. C. Williams, Pleiotropy, Natural Selection and the Evolution of Senescence. *Evolution.* **11**, 398–411 (1957).

16. W. D. Hamilton, The moulding of senescence by natural selection. *J. Theor. Biol.* **12**, 12–45 (1966).

17. M. Ackermann, S. C. Stearns, U. Jenal, Senescence in a Bacterium with Asymmetric Division. *Science.* **300**, 1920 (2003).

18. E. J. Stewart, R. Madden, G. Paul, F. Taddei, Aging and death in an organism that reproduces by morphologically symmetric division. *PLoS Biol.* **3**, e45 (2005).

19. N. Erjavec, M. Cvijovic, E. Klipp, T. Nyström, Selective benefits of damage partitioning in unicellular systems and its effects on aging. *Proc. Natl. Acad. Sci. U. S. A.* **105**, 18764–18769 (2008).

20. S. R. Laney, R. J. Olson, H. M. Sosik, Diatoms favor their younger daughters. *Limnol. Oceanogr.* **57**, 1572–1578 (2012).

21. C. U. Rang, A. Y. Peng, L. Chao, Temporal dynamics of bacterial aging and rejuvenation. *Curr. Biol.* **21**, 1813–6 (2011).

22. U. K. Steiner, *et al.*, Two stochastic processes shape diverse senescence patterns in a single-cell organism. *Evolution.* **73**, 847–857 (2019).

23. A. M. Proenca, C. U. Rang, A. Qiu, C. Shi, L. Chao, Cell aging preserves cellular immortality in the presence of lethal levels of damage. *PLOS Biol.* **17**, e3000266 (2019).

24. M. Tuğrul, U. K. Steiner, Demographic Consequences of Damage Dynamics in Single-Cell Ageing. *bioRxiv* (2023) https:/doi.org/10.1101/2023.05.23.538602.

25. T. B. L. Kirkwood, Understanding ageing from an evolutionary perspective. *J. Intern. Med.* **263**, 117–127 (2008).

26. L. Chao, A model for damage load and its implications for the evolution of bacterial aging. *PLoS Genet.* **6**, e1001076 (2010).

27. M. Ackermann, L. Chao, C. T. Bergstrom, M. Doebeli, On the evolutionary origin of aging. *Aging Cell* **6**, 235–44 (2007).

28. A. B. Lindner, R. Madden, A. Demarez, E. J. Stewart, F. Taddei, Asymmetric segregation of protein aggregates is associated with cellular aging and rejuvenation. *Proc. Natl. Acad. Sci. U. S. A.* **105**, 3076–81 (2008).

29. A. B. Lindner, A. Demarez, Protein aggregation as a paradigm of aging. *Biochim. Biophys. Acta - Gen. Subj.* **1790**, 980–996 (2009).

30. A. S. Coquel, *et al.*, Localization of Protein Aggregation in Escherichia coli Is Governed by Diffusion and Nucleoid Macromolecular Crowding Effect. *PLoS Comput. Biol.* **9** (2013).

31. J. Winkler, *et al.*, Quantitative and spatio-temporal features of protein aggregation in Escherichia coli and consequences on protein quality control and cellular ageing. *EMBO J.* **29**, 910–23 (2010).

32. S. K. Govers, J. Mortier, A. Adam, A. Aertsen, Protein aggregates encode epigenetic memory of stressful encounters in individual Escherichia coli cells. *PLOS Biol.* **16**, e2003853 (2018).

33. U. Łapińska, G. Glover, P. Capilla-Lasheras, A. J. Young, S. Pagliara, Bacterial ageing in the absence of external stressors. *Philos. Trans. R. Soc. B Biol. Sci.* **374** (2019).

34. D. Steinsaltz, M. D. Christodoulou, A. A. Cohen, U. K. Steiner, *Chance events in aging* (Elsevier Inc., 2019).

35. O. K. Silander, *et al.*, A genome-wide analysis of promoter-mediated phenotypic noise in Escherichia coli. *PLoS Genet.* **8** (2012).

36. C. Shi, *et al.*, Allocation of gene products to daughter cells is determined by the age of the mother in single Escherichia coli cells. *Proc. R. Soc. B* **287**, 20200569 (2020).

37. A. Battesti, N. Majdalani, S. Gottesman, The RpoS-mediated general stress response in escherichia coli. *Annu. Rev. Microbiol.* **65**, 189–213 (2011).

38. R. Lange, R. Hengge-Aronis, Identification of a central regulator of stationary-phase gene expression in Escherichia coli. *Mol. Microbiol.* **5**, 49–59 (1991).

39. H. Weber, T. Polen, J. Heuveling, V. F. Wendisch, R. Hengge, Genome-wide analysis of the general stress response network in Escherichia coli: σS-dependent genes, promoters, and sigma factor selectivity. *J. Bacteriol.* **187**, 1591–1603 (2005).

40. P. Wang, *et al.*, Robust growth of Escherichia coli. *Curr. Biol.* **20**, 1099–103 (2010).

41. S. Taheri-Araghi, *et al.*, Cell-Size Control and Homeostasis in Bacteria. *Curr. Biol.* **25**, 385–391 (2015).

42. S. N. Evans, D. Steinsaltz, Damage segregation at fissioning may increase growth rates: A superprocess model. *Theor. Popul. Biol.* **71**, 473–490 (2007).

43. Y. Yang, *et al.*, Temporal scaling of ageing as an adaptive strategy of Escherichia coli. *Sci. Adv.* **5**, eaaw2069 (2019).

44. L. Chao, C. K. Chen, C. Shi, C. U. Rang, Spatial and temporal distribution of ribosomes in single cells reveals aging differences between old and new daughters of Escherichia coli.

bioRxiv (2023) https:/doi.org/10.1101/2023.06.21.545935.

45. A. Zaslaver, *et al.*, A comprehensive library of fluorescent transcriptional reporters for Escherichia coli. *Nat. Methods* **3**, 623–628 (2006).

46. J. B. Lugagne, H. Lin, M. J. Dunlop, Delta: Automated cell segmentation, tracking, and lineage reconstruction using deep learning. *PLoS Comput. Biol.* **16**, 1–18 (2020).

47. R Core Team, R: A language and environment for statistical computing (2017).

48. S. N. Wood, Fast stable restricted maximum likelihood and marginal likelihood estimation of semiparametric generalized linear models. *J. R. Stat. Soc. Ser. B Stat. Methodol.* **73**, 3–36 (2011).

49. K. P. Burnham, D. R. Anderson, Multimodel inference: Understanding AIC and BIC in model selection. *Sociol. Methods Res.* **33**, 261–304 (2004).

50. V. M. R. Muggeo, Estimating regression models with unknown break-points. *Stat. Med.* **22**, 3055–3071 (2003).